

Shortcomings of the standard Lennard–Jones dispersion term in water models, studied with force matching

Paolo Nicolini, Elvira Guàrdia, and Marco Masia

Citation: *The Journal of Chemical Physics* **139**, 184111 (2013); doi: 10.1063/1.4829444

View online: <http://dx.doi.org/10.1063/1.4829444>

View Table of Contents: <http://scitation.aip.org/content/aip/journal/jcp/139/18?ver=pdfcov>

Published by the [AIP Publishing](#)



Re-register for Table of Content Alerts

Create a profile.



Sign up today!



Shortcomings of the standard Lennard–Jones dispersion term in water models, studied with force matching

Paolo Nicolini,^{1,2,a)} Elvira Guàrdia,^{1,b)} and Marco Masia^{3,c)}

¹Departament de Física i Enginyeria Nuclear, Universitat Politècnica de Catalunya, Campus Nord B4-B5, Barcelona 08034, Spain

²Department of Control Engineering, Faculty of Electrical Engineering, Czech Technical University in Prague, Technická 2, 16627 Prague 6, Czech Republic

³Dipartimento di Chimica, Università degli Studi di Sassari, Istituto Officina dei Materiali del CNR, UOS SLACS, Via Vienna 2, 07100 Sassari, Italy

(Received 22 July 2013; accepted 23 October 2013; published online 12 November 2013)

In this work, *ab initio* parametrization of water force field is used to get insights into the functional form of empirical potentials to properly model the physics underlying dispersion interactions. We exploited the force matching algorithm to fit the interaction forces obtained with dispersion corrected density functional theory based molecular dynamics simulations. We found that the standard Lennard-Jones interaction potentials poorly reproduce the attractive character of dispersion forces. This drawback can be resolved by accounting for the distinctive short range behavior of dispersion interactions, multiplying the r^{-6} term by a damping function. We propose two novel parametrizations of the force field using different damping functions. Structural and dynamical properties of the new models are computed and compared with the ones obtained from the non-damped force field, showing an improved agreement with reference first principle calculations. © 2013 AIP Publishing LLC. [<http://dx.doi.org/10.1063/1.4829444>]

I. INTRODUCTION

The Holy Grail in the development of empirical potentials is the use of simple functional forms, as they are implemented in the most widespread general purpose molecular dynamics (MD) simulation packages, and they are relatively simple to parametrize. Probably, the Lennard-Jones potential (LJ) is the most used, either in the σ - ε or in the A - C forms

$$U_{LJ}(r) = 4\varepsilon \left[\left(\frac{\sigma}{r} \right)^{12} - \left(\frac{\sigma}{r} \right)^6 \right] = \frac{A}{r^{12}} - \frac{C}{r^6}. \quad (1)$$

Given that $A = 4\varepsilon\sigma^{12}$ and $C = \varepsilon\sigma^6$, the two formulations are fully equivalent, but they bear different physical meanings of the two parameter sets: in the former, ε and σ represent, respectively, the depth of the potential well and the finite inter-particle distance at which the potential is zero; whereas the latter form allows an understanding of the interactions in terms of short range repulsion (A) and van der Waals attraction (C). In case of atomic liquids, the last term expresses the dispersive interaction and it is proportional to the product of polarizabilities and, as such, it is always attractive. For polar liquids, this parameter accounts also for dipole-dipole interactions (and induction, for mixtures of polar and polarizable particles) that depend on the dipoles angular orientation; nevertheless, considering the Boltzmann average over different rotational orientations, the overall C/r^6 effect has to be attractive.¹

In recent parametrizations of force fields (FF) from *ab initio* reference data,^{2–6} some of the LJ C coefficients assume negative values. Such a repulsive “dispersion” term is usually compensated by an increase of the electrostatic attraction due to slightly overestimated partial charges. Even if some explanations of these results are attempted (see, for example, comments on the short-range interaction potential in Ref. 2), in our opinion, a deeper analysis is due, in order to clarify some blurry aspects. All the above mentioned results have been obtained using sophisticated calculations based on the force matching (FM) algorithm, a method developed and successfully applied by Ercolessi and Adams⁷ to derive a glue potential for Al. Roughly speaking, FM is based on fitting the effective potential parameters to reference atomic forces. Practically, the task consists on the minimization of a proper penalty function, usually obtained as an accumulation over many configurations and/or many particles of the least square differences between reference and effective physical quantities (originally only forces). Recently, the method has been applied for parametrizing classical force fields of a wide variety of systems, particularly water,^{2–6,8–16} taking advantages also from new smarter implementations.^{2,16}

In this work, we will show that it is possible to systematically use the FM method to properly account for the dispersion interaction, and to obtain deeper insights on its nature. The paper is organized as follows: in Sec. II, we discuss the main features of the matching algorithm (Sec. II A), the damping functions employed (Sec. II B), and we give the computational details for density functional theory (DFT) (Sec. II C) and classical MD (Sec. II D) simulations. Results and conclusions are discussed, respectively, in Secs. III and IV.

^{a)}Electronic mail: nicolpao@fel.cvut.cz

^{b)}Electronic mail: elvira.guardia@upc.edu

^{c)}Electronic mail: marco.masia@uniss.it. Present address: Institut für Physikalische und Theoretische Chemie, Goethe Universität Frankfurt, Max-von-Laue-Str. 7, D-60438 Frankfurt am Main, Germany.

II. METHODS AND COMPUTATIONAL DETAILS

A. The FM algorithm

In this work, we exploited the FM approach in order to parametrize empirical FF for water. This was done performing a least square fitting on reference DFT data. We performed a minimization in the parameter space of the following penalty function:

$$\chi^2 = \sum_{i=1}^{N_{conf}} \sum_{A=F,\tau} \sum_{j=1}^{N_{mol}} w(A_{i,j}^{DFT}, \beta_A) (A_{i,j}^{FF} - A_{i,j}^{DFT})^2, \quad (2)$$

$$w(A_{i,j}^{DFT}, \beta_A) = \frac{|A_{i,j}^{DFT}|^{\beta_A}}{\sum_{j'=1}^{N_{mol}} |A_{i,j'}^{DFT}|^{\beta_A+2}},$$

where N_{conf} is the total number of configurations used in the fitting, N_{mol} is the number of molecules in the simulation box, $A_{i,j}$ represents the components of net molecular forces (F) and torques (τ) acting on the center of mass of the j th molecules in the i th configuration, and w is the weight used to account for the different magnitude (and physical units) of forces and torques. β_A are positive integers that allow us to have some flexibility in the weighting. To set β_A to 0 means that we are applying only the normalizing factor, while when $\beta_A \neq 0$ more importance is given to the configurations (and to the molecules) with large values of A . In order to make possible a comparison with the force fields previously reported, the choice of the β values was done following Ref. 6. For the minimization, we used a quadratic polynomial interpolation line-search directions found using the Broyden-Fletcher-Goldfarb-Shanno formula.¹⁷ To rule out the existence of different minima in the penalty function that would lead to distinct parameter sets, we performed many minimizations, starting from different initial conditions. We checked that all of them converged to one single minimum.

B. Damping functions

The dispersion attraction is due to the many-body interactions between charge distributions: the fluctuations due to the electrons movement on different molecules become correlated and the overall effect is to lower the total energy; thus, this interaction that is intrinsically long ranged, is always attractive.¹⁸ At short distances, due to the spatial distribution of the molecular electronic densities, the interaction is damped,^{11,19} and thus the C/r^6 term in Eq. (1) might also be damped. Both in the case of explicitly accounting for dipolar interactions (see, for example, polarizable force fields¹¹), or in the case of empirical corrections to DFT calculations,^{20–28} it is common practice to use damping functions to switch to zero the interaction at short distances. The use of these functions has been thoroughly justified on physically sound arguments.¹⁸ Therefore, we hereby explore the consequences of damping or not the LJ dispersion parameter in the water-water force fields. To this end, we cast the intermolecular po-

tential in the general form

$$U = \sum_{j<i}^{N_o} \left[\frac{A_{oo}}{r_{ij}^{12}} - f(r_{ij}) \frac{C_{oo}}{r_{ij}^6} \right] + \frac{1}{4\pi\epsilon_0} \sum_{j<i}^N \frac{q_i q_j}{r_{ij}}, \quad (3)$$

where the first sum runs over the oxygen atoms, while the latter refers to all atom pairs from atoms in different molecules. $f(r)$ is a generic damping function that describes the short-range penetration correction to the asymptotic expansion of dispersion.²⁹ Necessary but not sufficient requirements are that $f(r)$ has the correct asymptotic behavior ($\lim_{r \rightarrow \infty} = 1$ and $\lim_{r \rightarrow 0} = 0$), and that it dominates over the r^{-6} term at short distances. Among the several types of damping functions present in the literature,^{20–23,28} we will make use of two of the most employed.^{14,20,23–27,30–32} The first one is a Fermi-like (FE) function^{23,46}

$$f(r) = \frac{1}{1 + \exp[-b(r/r_0 - 1)]} \quad (4)$$

that was used, among others, by Grimme²⁴ for calculating the dispersion corrections in the DFT-D scheme. The two free parameters b and r_0 represent, respectively, the steepness and the range where the damping is applied. The second damping function employed was proposed by Tang and Toennies (TT),²⁰ proven to reproduce the correct behavior for rare gas dimers³⁰

$$f(r) = 1 - \exp(-br) \sum_{k=0}^6 \frac{(br)^k}{k!}. \quad (5)$$

It contains only one free parameter that determines shape and position of the damping. In order to have the same number of free parameters in the fit of the two damping functions, and following Ref. 23, we set the parameter r_0 of the Fermi function to 2.75 Å that is the value of the molecular radius of water in the condensed phase.³³

Three water models are presented in the following: the SPC/FM model of Ref. 6 (hereafter referred to as ND, stands for no-damping on the C parameter, i.e., $f(r) = 1$), while the other two are obtained using Fermi (FE, Eq. (4)) and Tang-Toennies (TT, Eq. (5)) damping functions. In all cases, we followed the matching procedure described in Sec. II A for optimizing A , C , and the partial charge on the oxygen atom. For FE and TT, at the same time, the parameter b was also optimized.

C. DFT simulations

Ab initio MD simulations were made using the Car-Parrinello scheme³⁴ for propagating the wavefunctions and the ionic configurations as implemented in the CPMD package.³⁵ The cutoff for the wavefunctions was set to 80 Ry, the time step was set to 4 a.u., and the fictitious mass for the orbital was chosen to be 400 amu. The BLYP density functional^{36,37} was used for the electronic structure calculations. The dispersion interactions have been taken into account using dispersion-corrected atom-centered pseudopotentials (DCACPs)^{38,39} in the Troullier-Martins format⁴⁰ for oxygen and hydrogen. Contrary to what is done in the DFT-D scheme of Grimme²⁴ where an empirical correction is

added *a posteriori*, using DCACPs the dispersion interaction is included in the pseudopotential, and hence, in the electron density resulting from the electronic structure calculation. It has been shown that these pseudopotentials successfully account for dispersion forces, and that they are capable of faithfully reproducing many dynamical and structural properties of water.³⁹

A cubic simulation box containing 96 water molecules at the density of 0.997 g cm^{-3} was used. Periodic boundary conditions were applied. The initial configurations were generated with classical MD simulations of 200 ps using the SPC/E model of water. Following Lin *et al.*,³⁹ we then performed a NVT ($T = 330 \text{ K}$) equilibration run of 3 ps, followed by a run of 15 ps in the microcanonical ensemble during which time we stored atomic positions and forces every 230 time step for a total of 600 configurations. The temperature was set to 330 K in order to avoid falling into the temperature range where BLYP simulations suffer for non-ergodic behavior⁴¹ on time scales shorter than 20 ps.

D. Classical MD

The empirical water models used are rigid and with fixed charges on oxygen and hydrogen atoms. While the charge values are obtained from the FM procedure, O–H bond length and H–O–H bending angle are kept fixed to the average values obtained from DFT simulations (0.995 \AA and 105.6° , respectively). With this geometry and after obtaining the explicit values of the force field parameters, we ran MD simulations using the different models to check how they compare with the reference first principle simulations. To this end, six independent randomly generated configurations of 96 molecules have been equilibrated for 500 ps in the canonical ensemble with the same side-length of the cubic box as the one used for reference DFT calculations. The temperature was set to 330 K to reproduce the same conditions of our DFT simulations. The Ewald summation technique⁴² was used to account for electrostatic interactions in periodic systems. For each run, we performed 1 ns of subsequent MD simulation in the NVE ensemble. Structural and dynamical properties were then computed and averaged over the six systems. In particular, we have computed radial distribution functions (RDFs), diffusion coefficients, and rotational characteristic times of relaxation for the O–H and H–H vectors, and compared the results to DFT simulations.

III. RESULTS AND DISCUSSION

The results of the parametrization are reported in Table I. It can be noticed that, by including a damping function in the interaction potential, the C parameters have positive values, thus recovering the expected physical behavior. The dispersion interaction is smoothly switched on as the distance increases, and it is fully reproduced at long range, where it is meaningful. On the other hand, for short and intermediate distances, its contribution is less effective. We stress that C becomes positive regardless of the type of damping function used, thus confirming the trend expected by our ar-

TABLE I. Parameters of the force fields obtained via FM adding the damping functions in Eqs. (4) and (5) into the LJ potentials. The units of b are \AA^{-1} in the case of TT damping, and dimensionless in the case of FE damping.

	ND ⁶	FE	TT
q_O (e)	−0.884	−0.878	−0.881
A_{OO} ($10^3 \text{ kcal mol}^{-1} \text{\AA}^{12}$)	377.743	478.881	533.722
C_{OO} ($\text{kcal mol}^{-1} \text{\AA}^6$)	−1319.455	493.883	287.224
b	...	33.1	0.762

guments. Notably, our parameters are in qualitative agreement with the one obtained independently by Rotenberg and co-workers,³¹ using the approach developed by Silvestrelli,²⁷ based on the spread of Wannier orbitals. In Table I, we also notice that, as the dispersive term becomes positive, the repulsive wall becomes steeper: the value of A increases more than $10^5 \text{ kcal mol}^{-1} \text{\AA}^{12}$ by passing from the ND model to FE. This increase is justified by the fact that in the ND model C contributes to the repulsion interaction, and A does not need to be high. The feature of reproducing the correct sign (i.e., the attractive nature) of the dispersion term is exactly the result that we are looking for and it resolves in itself the issue that we addressed.

In order to further assess the quality of the FM procedure, we calculate the percent normalized root mean square deviation (NRMSD_%) of the classical target properties from the reference ones using the following:

$$\text{NRMSD}_{\%}(A) = \frac{\sqrt{\frac{1}{N_{\text{conf}} N_{\text{mol}}} \sum_{i=1}^{N_{\text{conf}}} \sum_{j=1}^{N_{\text{mol}}} (A_{i,j}^{\text{FF}} - A_{i,j}^{\text{DFT}})^2}}{\max_{i,j} \{A_{i,j}^{\text{DFT}}\} - \min_{i,j} \{A_{i,j}^{\text{DFT}}\}} \cdot 100, \quad (6)$$

where $A = F, \tau$. We introduce this quantity in place of the RMSD, because it eases the comparison between different quantities. We would like to stress that the absolute values of χ^2 obtained during minimization cannot be used to compare distinct force fields.⁶ Results for the three models are reported in Table II. The main outcome is that none of the effective interaction potentials is able to perfectly reproduce the reference DFT forces and torques, even adding the damping functions on the dispersion part. This is due to the extreme simplicity of the chosen model (i.e., rigid molecules, fixed charges, only pairwise interactions considered). Anyway, it is possible to note some improvement in both the damped force fields respect of the non-damped one, especially for net molecular forces. In particular, among the three, FE model seems to provide the best behavior.

Although these differences may seem tiny, we observed a relevant improvement of the resulting force fields. The

TABLE II. Normalized percent RMSD of net molecular forces and torques for damped and non-damped force fields.

	ND ⁶	FE	TT
NRMSD _% (F)	8.18	7.81	8.08
NRMSD _% (τ)	9.13	9.05	9.07

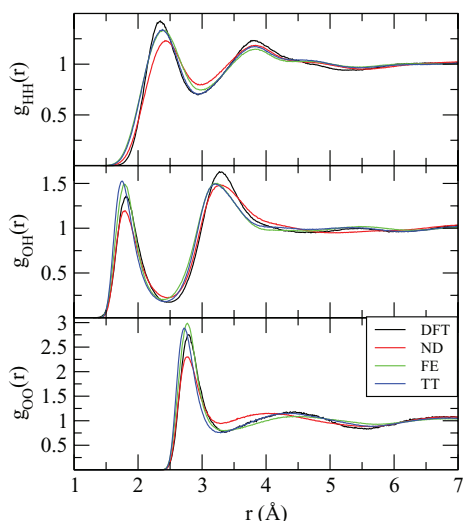


FIG. 1. Atom-atom radial distribution functions for all potential models and for the reference DFT simulations.

atom-atom RDFs are shown in Figure 1. The ND model poorly reproduces the main structural features of the DFT reference calculations. Both positions and amplitude of the peaks are offset for the RDFs of all atom pairs. On the other hand, the damped models perform better, particularly for the oxygen-oxygen RDF. Although an improvement is also seen for the O–H and H–H RDFs, all the models are not good enough to reproduce the DFT results. This is due to the fact that the force fields used account only for LJ interactions among oxygens; a better reproduction of all structural properties would require the parametrization of a more complex interaction potential, which is out of the scope of this paper. It is remarkable, though, that the use of a proper form for the dispersion interaction between oxygens yields improved structures for all atom pairs.

Dynamical properties are shown in Figure 2. The diffusion coefficients (D) were obtained by the slope of the mean square displacement. The characteristic times for rotational relaxation (τ) were computed by fitting the tails of the exponentially decaying rotational autocorrelation functions, obtained as first and second Legendre polynomials of the vectors joining O–H and H–H.⁴³ In the first panel of Figure 2, we show the comparison between the diffusion coefficients

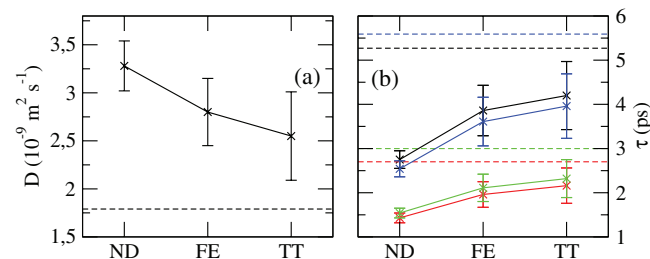


FIG. 2. Comparison between reference and calculated dynamical properties. Reference values are plotted with horizontal dashed lines. Panel (a) Diffusion coefficients. Panel (b) Characteristic rotational times for first and second Legendre polynomials. Black and red represent the O–H vector, while blue and green are used for the H–H vector. In both panels, lines connecting the points are guides for the eye.

obtained with the three classical models and the one obtained with DFT simulations. It can be seen that the damped models are in better agreement with the reference value, in particular TT. The same trend is found for the rotational times obtained by first and second Legendre polynomials.

As discussed above, a better agreement between reference calculations and our models would be obtained using a more complete interaction potential. It is worth noticing that the improved performance of the damped force fields could be ascribed to an increase in the parameter space dimension, and in a different functional form of the empirical potential that allow for more flexibility in the fitting procedure. Nonetheless, we would like to stress that the important change introduced herein consists in modifying the standard LJ potential to properly describe the nature of dispersion interactions. This is indeed the most remarkable result of our calculations. If the dispersion interaction is not properly damped at short range, the fitting procedure converges to negative values for C . This is not due to artifacts of the optimization algorithm, but rather to a shortcoming of the LJ potentials. In fact, the set of parameters found is the best that could reproduce most of the interactions in the system. The poor description of the dispersion interaction is clearly reflected in a looser structure in the RDFs. The greater closeness between calculated and reference properties obtained with damped models is a clear signal that the physics of the system is better reproduced. During the development of this work, many attempts have been devoted to check the effect of model modifications on the overall results. In fact, we have tried to use more complex LJ potentials with interaction sites located also on the hydrogens and even to change the geometry of the interaction sites by moving the negative charge on a ghost atom along the H–O–H angle bisector (in a fashion similar to the well-known TIP4P model⁴⁴). None of these exploratory tests produced positive dispersion parameter (see the supplementary material⁴⁵). The fact that these models possess a larger number of parameters than FE and TT and still do not predict the correct sign of the C parameter, strongly support the conclusion that the improvements showed by our new models cannot be ascribed to the bigger flexibility of FE and TT respect ND. In other words, what appears from our results is that what really matters is not the number of parameters, but rather a proper description of the underlying physics.

IV. CONCLUDING REMARKS

In this paper, we applied the force matching algorithm to parametrize new force fields for water. This is done fitting reference DFT based calculation and optimizing the parameter values of the model. Particular attention was paid for the treatment of dispersion. In fact, starting from recent papers where the attractive nature of this interaction was poorly reproduced, we showed that an improved description could be achieved including a damping function in the r^{-6} term. In addition, we calculated structural and dynamical properties for the new models (such as pair radial distribution functions, diffusion coefficient, and orientational characteristic times). We found that the results obtained from these models are in

better agreement with the reference DFT data respect of the ones obtained from the non-damped model.

The most important consequence of our results is that *any* empirical potential based on the standard Lennard-Jones potential (i.e., without damping), does not give a realistic description of the system. In fact, simply looking at the dispersion part of the non-damped Lennard-Jones potential, while on the one hand it can describe properly the long range attraction, on the other hand it provides wrong predictions of the behavior at short distances (or vice versa). Accordingly, the “optimal” C value will be a compromise between a short-range overestimation and a long-range underestimation, preventing so the possibility of giving an accurate description of the interaction over the entire spatial extent. Therefore, although existing Lennard-Jones based force fields for water (and for any other molecular liquid) are quite good and are able to describe some of the experimental properties, we are convinced that an improved description would be obtained only by including a short range damping of the dispersion interaction. This might be of particular importance for those applications aimed at studying the collective or macroscopic behaviors originating from atomistic interactions.

ACKNOWLEDGMENTS

The authors thankfully acknowledge the computer resources, technical expertise, and assistance provided by the Barcelona Supercomputing Center – Centro Nacional de Supercomputación for Project Nos. QCM-2009-1-0014, QCM-2008-3-0012, and QCM-2008-2-0010. E.G. acknowledges financial support from the Spanish MINECO (Grant No. FIS2012-39443-C02-01) and from the Government of Catalonia (Grant No. 2009SGR-1003). M.M. acknowledges funding from the EU Marie Curie Fellowship programme FP7-PEOPLE-2011-IOF (Contract No. PEOF-GA-2011-299345), as well as funding from the University of Sassari. P.N. acknowledges financial support from Grant No. CZ.1.07/2.3.00/30.0034.

- ¹P. Atkins and J. de Paula, *Physical Chemistry*, 8th ed. (Oxford University Press, 2006).
- ²O. Akin-Ojo, Y. Song, and F. Wang, *J. Chem. Phys.* **129**, 064108 (2008).
- ³O. Akin-Ojo and F. Wang, *J. Phys. Chem. B* **113**, 1237 (2009).
- ⁴J. Sala, E. Guàrdia, and M. Masia, *Comput. Phys. Commun.* **182**, 1954 (2011).
- ⁵D. Spångberg, E. Guàrdia, and M. Masia, *Comput. Theor. Chem.* **982**, 58 (2012).
- ⁶J. Sala, E. Guàrdia, J. Martí, D. Spångberg, and M. Masia, *J. Chem. Phys.* **136**, 054103 (2012).
- ⁷F. Ercolessi and J. B. Adams, *Europhys. Lett.* **26**, 583 (1994).
- ⁸S. Izvekov, M. Parrinello, C. J. Burnham, and G. A. Voth, *J. Chem. Phys.* **120**, 10896 (2004).
- ⁹S. Izvekov and G. A. Voth, *J. Chem. Phys.* **123**, 134105 (2005).
- ¹⁰Y. Song, O. Akin-Ojo, and F. Wang, *J. Chem. Phys.* **133**, 174115 (2010).

- ¹¹J. Sala, E. Guàrdia, and M. Masia, *J. Chem. Phys.* **133**, 234101 (2010).
- ¹²O. Akin-Ojo and F. Wang, *J. Comput. Chem.* **32**, 453 (2011).
- ¹³F. Wang, O. Akin-Ojo, E. Pinnick, and Y. Song, *Mol. Simul.* **37**, 591 (2011).
- ¹⁴S. Tazi, J. J. Molina, B. Rotenberg, P. Turq, R. Vuilleumier, and M. Salanne, *J. Chem. Phys.* **136**, 114507 (2012).
- ¹⁵C. Pinilla, A. H. Irani, N. Seriani, and S. Scandolo, *J. Chem. Phys.* **136**, 114511 (2012).
- ¹⁶L.-P. Wang, J. Chen, and T. Van Voorhis, *J. Chem. Theory Comput.* **9**, 452 (2013).
- ¹⁷J. Nocedal and S. J. Wright, *Numerical Optimization*, 2nd ed. (Springer, New York, 2006).
- ¹⁸A. J. Stone, *The Theory of Intermolecular Forces*, International Series of Monographs on Chemistry Vol. 32 (Oxford University Press, Oxford, 1996).
- ¹⁹M. Masia, M. Probst, and R. Rey, *J. Chem. Phys.* **123**, 164505 (2005).
- ²⁰K. T. Tang and J. P. Toennies, *J. Chem. Phys.* **80**, 3726 (1984).
- ²¹W. T. M. Mooij, F. B. van Duijneveldt, J. G. C. M. van Duijneveldt-van de Rijdt, and B. P. van Eijck, *J. Phys. Chem. A* **103**, 9872 (1999).
- ²²M. Elstner, P. Hobza, T. Frauenheim, S. Suhai, and E. Kaxiras, *J. Chem. Phys.* **114**, 5149 (2001).
- ²³Q. Wu and W. Yang, *J. Chem. Phys.* **116**, 515 (2002).
- ²⁴S. Grimme, *J. Comput. Chem.* **25**, 1463 (2004).
- ²⁵S. Grimme, *J. Comput. Chem.* **27**, 1787 (2006).
- ²⁶P. Jurecka, J. Cerny, P. Hobza, and D. R. Salahub, *J. Comput. Chem.* **28**, 555 (2007).
- ²⁷P. L. Silvestrelli, *Phys. Rev. Lett.* **100**, 053002 (2008).
- ²⁸Y. Liu and W. A. Goddard III, *Mater. Trans.* **50**, 1664 (2009).
- ²⁹M. Salanne, L. J. A. Siqueira, A. P. Seitsonen, P. A. Madden, and B. Kirchner, *Faraday Discuss.* **154**, 171 (2012).
- ³⁰K. T. Tang and J. P. Toennies, *J. Chem. Phys.* **118**, 4976 (2003).
- ³¹B. Rotenberg, M. Salanne, C. Simon, and R. Vuilleumier, *Phys. Rev. Lett.* **104**, 138301 (2010).
- ³²M. Salanne, B. Rotenberg, S. Jahn, R. Vuilleumier, C. Simon, and P. A. Madden, *Theor. Chem. Acc.* **131**, 1143 (2012).
- ³³Y. Zhang and Z. Xu, *Am. Mineral.* **80**, 670 (1995).
- ³⁴R. Car and M. Parrinello, *Phys. Rev. Lett.* **55**, 2471 (1985).
- ³⁵CPMD, see <http://www.cpmid.org>, Copyright IBM Corp 1990–2008, Copyright MPI für Festkörperforschung Stuttgart 1997–2001.
- ³⁶A. D. Becke, *Phys. Rev. A* **38**, 3098 (1988).
- ³⁷C. Lee, W. Yang, and R. G. Parr, *Phys. Rev. B* **37**, 785 (1988).
- ³⁸O. A. von Lilienfeld, I. Tavernelli, U. Rothlisberger, and D. Sebastiani, *Phys. Rev. Lett.* **93**, 153004 (2004).
- ³⁹I.-C. Lin, A. P. Seitsonen, M. D. Coutinho-Neto, I. Tavernelli, and U. Rothlisberger, *J. Phys. Chem. B* **113**, 1127 (2009).
- ⁴⁰N. Troullier and J. L. Martins, *Phys. Rev. B* **43**, 1993 (1991).
- ⁴¹I.-F. W. Kuo, C. J. Mundy, M. J. McGrath, J. I. Siepmann, J. VandeVondele, M. Sprik, J. Hutter, B. Chen, M. L. Klein, F. Mohamed, M. Krack, and M. Parrinello, *J. Phys. Chem. B* **108**, 12990 (2004).
- ⁴²P. P. Ewald, *Ann. Phys. (Berlin)* **369**, 253 (1921).
- ⁴³E. Guàrdia, A. M. Calvo, and M. Masia, *Theor. Chem. Acc.* **131**, 1152 (2012).
- ⁴⁴W. L. Jorgensen, J. Chandrasekhar, J. D. Madura, R. W. Impey, and M. L. Klein, *J. Chem. Phys.* **79**, 926 (1983).
- ⁴⁵See supplementary material at <http://dx.doi.org/10.1063/1.4829444> for exploratory tests on models with LJ sites located on hydrogen atoms and with negative charge located on a ghost atom along the H–O–H angle bisector.
- ⁴⁶Note that the FE function seems not able to dominate the divergent behavior of the r^{-6} term and even that it does not converge to zero for $r \rightarrow 0$ (i.e., it goes to some small but finite value). For these reasons, apparently FE does not meet the necessary conditions stated in Sec. II B. Nevertheless, looking at the explicit parametrization given in Table I, it is possible to show that, *as matter of fact*, the FE function switches to zero the dispersion interaction in a wide region between r_0 and 0, as expected for a damping function.